A "Failed" Assay Development for the Discovery of Rescuing Small Molecules from the Radiation Damage

Kuo-Kuang Wen[1], Stephen Roy[2], Isabella M. Grumbach[2], and Meng Wu[1,3,4] iD

Abstract

With improving survival rates for cancer patients, the side effects of radiation therapy, especially for pediatric or more sensitive adult patients, have raised interest in preventive or rescue treatment to overcome the detrimental effects of efficient radiation therapies. For the discovery of rescuing small molecules for radiation damage to the endothelium, we have been developing a 96-well microplate-based in vitro assay for high-throughput compatible measurement of radiation-induced cell damage and its rescue by phenotypic high-content imaging. In contrast to traditional radiation assays with detached cells for clonogenic formation, we observed cells with live-cell imaging in two different kinds of endothelial cells, up to three different cell densities, two gamma-infrared radiation dose rates, more than four different radiation doses, and acute (within 24 h with one to two h intervals) and chronic (up to 7 days) responses by phenotypic changes (digital phase contrast) and functional assays (nuclear, live-cell, and dead-cell staining) at the end of the assay. Multiple potential small molecules, which have been reported for rescuing radiation damage, have been tested as assay controls with dose responses. At the end, we did not move ahead with the pilot screening. The lessons learned from this "failed" assay development are shared.

Keywords

Introduction

Assay development, especially for high-throughput screening, is a tough business.[1] Usually the challenges, known as the "valley of death" of the drug discovery process,[2,3] are attributed to the nonperfect in vitro assays for early drug discovery. The robustness, biology/physiology relevance, and automation compatibility (microplate based) of the assays are to be optimized to generate hits that ultimately can be used/developed for in vivo and clinical application.[4] These three factors also greatly limit the available in vitro models[5,6] and the windows of the signals[7,8] in assay development, despite there being a plethora of target-based and phenotypic assays that have been developed for early drug discovery and systems biology research.[9,10] Here we present a "failed" assay development for the discovery of small molecules that rescue or mitigate radiation damage in noncancerous tissue. This example, in contrast, demonstrates the complications and difficulties that can arise during assay development.

Radiation therapy for cancer[11] has been part of standard treatment for 50% of cancer patients, in addition to surgery, chemotherapy, and, more recently, immunotherapy.[12] Because of the continuingly improving survival rate of

[1]University of Iowa High Throughput Screening (UIHTS) Core, University of Iowa, Iowa City, IA, USA
[2]Division of Cardiovascular Medicine, Department of Internal Medicine, Abboud Cardiovascular Research Center, Carver College of Medicine, University of Iowa, Iowa City, IA, USA
[3]Department of Biochemistry, Carver College of Medicine, University of Iowa Iowa City, IA, USA
[4]Department of Pharmaceutical Sciences and Experimental Therapeutics, Division of Medicinal and Natural Products Chemistry, College of Pharmacy, University of Iowa, Iowa City, IA, USA

Corresponding Author:
Meng Wu, Department of Pharmaceutical Sciences and Experimental Therapeutics, Division of Medicinal and Natural Products Chemistry, College of Pharmacy, University of Iowa, 115 S Grand Ave 316 PHAR, Iowa City, IA 52242, USA.
Email: meng-wu@uiowa.edu

cancer patients, the long-term consequences of this primary treatment have emerged as a significant risk factor,[13] especially on the cardiovascular-related side effects.[14–16] Small-molecule drugs have been explored for rescuing radiation damage therapies for their transient, efficient, and biologically available characteristics. Recilisib sodium[17] (Ex-Rad) has been in a phase I trial as the only known oral radioprotectant. There are five major categories of reported irradiation rescue effects: (1) antioxidants or anti-inflammatory (e.g., auranofin,[18] GC1149,[19] or Mito-TEMPO[20]); (2) 8-oxoguanine glycosylase (OGG) activators (e.g., V028-5832[21] or melatonin[22]); (3) GPX4 activators through ferroptosis (Y600-0815[23] or ($\pm$)-α-tocopherol acetate[24] as a vitamin E analog); (4) hits/leads from whole-animal irradiation experiments (e.g., recilisib sodium,[17] also known as Ex-Rad, and γ-tocotrienol[25]); and (5) others, for example, histone deacetylase (HDAC) inhibitors (trichostatin A[26]). However, there are no systematic studies on the rescuing molecules, especially on specific tissues/organs, for example, cardiac endothelium or brain microvascular endothelium. A high-throughput plate-based in vitro assay would greatly facilitate the discovery of rescuing small molecules from radiation damage. The abovementioned small-molecule compounds will be utilized as positive controls for the assay development.

Currently, most of the assays for the discovery of rescuing small molecules from radiation damage are (1) clonogenic formation assays of radiated detached cells and (2) in vivo (mostly through mouse) experiments. Both are limited by their throughput to do systematic unbiased study on radiation effects. A high-throughput plate-based in vitro assay would attest not only hypothesis-based (e.g., OGG activators) but also unbiased phenotypic cell-based (e.g., synergistic effects of two or more targets) discovery of small molecules for rescuing radiation damage.

In this report, we describe how we developed a 96-well microplate-based in vitro assay for the high-throughput measurement of radiation-induced cell damage and its rescue by phenotypic high-content imaging. In contrast to traditional radiation assays with detached cells for clonogenic formation, we observed cells with live-cell imaging in two different kinds of endothelial cells, with up to three different cell densities, at two gamma-infrared radiation dose rates, and at more than four different radiation doses, for acute (within 24 h with one to two h intervals) and chronic (up to 7 days) responses by phenotypic changes (digital phase contrast [DPC]) and functional assays (nuclear, live-cell, and dead-cell staining) at the end of the assay. Eleven reported small molecules have been tested with dose responses as controls. In the end, we did not move ahead with the pilot screening because we could not identify any potential radiation rescuer controls. The lessons learned from this failed assay development are discussed.

Materials and Methods

Chemicals and Reagents

Dactinomycin and piplartine were purchased from Selleck Chemicals (Houston, TX); melatonin,[22] trichostatin A,[26] γ-tocotrienol,[25] auranofin,[18] genistein,[27] and Mito-TEMPO[20] from Cayman Chemicals (Ann Arbor, MI); GC1149[19] from Galera Therapeutics (Malvern, PA); recilisib sodium (also named Ex-Rad)[17] from MedKoo Biosciences (Morrisville, NC); and V028-5832 (also named compound C)[21] and Y600-0815(also named PKUMDL-LC-101)[23] from Enamine (Monmouth Junction, NJ). The stock solutions of all these chemicals at 10 mM DMSO were prepared, unless specified otherwise.

Cell-permeable Hoechst 33342 dye and Calcein-AM were from Thermo Fisher Scientific (Waltham, MA). Stock solutions (1 and 2 mM; 1000$\times$) were prepared according to the vendor's instructions, respectively.

Cells and Cell Culture

All cells were incubated at 37 °C in a humidified atmosphere of 5% CO_2. An hCMEC/D3 BBB cell line from Millipore Sigma (Burlington, MA) was cultured in DMEM:F12 (Dulbecco's Modified Eagle's Medium nutrient mixture Ham's F-121 in a 1:1 mixture) supplemented with 10% filtered fetal bovine serum (FBS; 10:100 media), 100 U/mL penicillin/100 µg/mL streptomycin (1:100 media), sodium pyruvate (1:100 media), L-glutamine (2:100 media, unless media already contains L- glutamine, then add 1:100), and nonessential amino acids (2:100 media). Human umbilical vein endothelial cells (HUVECs) from the American Type Culture Collection (ATCC; Rockville, MD) were cultured in endothelial cell medium-basal (ECM-b) from Sciencell Research Laboratories (Carlsbad, CA). In the 500 mL of basal media we added a 25 mL tube of bovine serum, endothelial cell growth supplement (ECGS), and 5 mL of penicillin/streptomycin (P/S). HEC-50 cells from Dr. Kim Leslie and Dr. Xiangbing Meng were maintained in DMEM supplemented with 10% FBS and 1% P/S (all from Gibco BRL, Carlsbad, CA).

Radiation and Drug Treatment

Before radiation exposure, the cells were cultured in T75 flasks in less than 90% confluency before cell seeding with routine cell detachment/splitting and counting for each cell line. In most cases, unless otherwise specified, the cells were seeded onto 96-well microplates (PerkinElmer CellCarrier-96 Ultra microplates, tissue culture treated, black, 96-well with lid, Waltham, MA) at a cell density of either 2500 or 10,000 cells/well and incubated for 48 h to

ensure that the cells formed a high-density, confluent monolayer, but still separated at a low cell density.

The control compounds were prepared in a 96-well drug plate (Greiner, Monroe, NC, microplate, 96-well, polypropylene, U-bottom, natural) for the serial dilution (1:3 for 8 wells or 1:2 for 12 wells) of each control compound. The drugs were added 24 h, 4 h, or immediately before the irradiation treatment (unless otherwise specified) with a change of culture media using the Hamilton MicroLab Star liquid handling system (Reno, NV).

Irradiation was performed on the abovementioned 96-well microplates with the culture media, with or without control compound treatment in serial dilutions. Cells were irradiated from 0 up to 440 Gy x-rays in the Radiation and Free Radical Research Core, delivered with either a PANTAK HF-320 ortho volt x-ray unit or an Xstrahl small-animal radiation research platform (SARRP) unit with different dose rates and doses (Gy) as specified. Cells in complete culture medium in microplates were exposed to irradiation at 22 °C, usually within half an hour. Two approaches of irradiation were applied on the microplate irradiation: one was covered with lead metal plates so that one single SBS standard 96-well plate can be divided into three or four blocks with different doses by controls of the irradiation time; the other microplate was set up using one dose per plate.

The PerkinElmer Operetta High Content Imaging System was used to monitor microplates using DPC imaging at 1 h intervals during the first 12 h, followed by either 2 or 8 h intervals over 24 h, unless otherwise specified. Usually, each plate was imaged before irradiation as well (denoted as –1 or –2; negative here indicates hour[s] before irradiation). After 24 h, plates were imaged every 24 h, after the daily media change, up to 7 days. At the end of the experiment, all the plates were stained with Hoechst for nuclear staining, calcein-AM for live-cell staining, and/or ethidium homodimer for dead-cell staining. Three additional channels of excitation (360–400 nm) and emission (500–550 nm) for Hoechst, excitation (460–490 nm) and emission (500–550 nm) for calcein-AM, and excitation (520–550 nm) and emission (580–650 nm) for ethidium homodimer were imaged.

Image analysis was done by instrument-accompanying Harmony software for a single DPC channel or four (DPC, Hoechst, calcein-AM, and ethidium homodimer) channels. Nuclei and cells were selected for both the intensity of all channels and morphology studies. The responses of radiation doses, control compound doses, and time-courses were analyzed by individual wells and/or individual cells within the wells using Spotfire (TIBCO and PerkinElmer) software for the visualization of the data sets. In cases where there was a dose response, additional analysis was performed with GraphPad Prism 9 (San Diego, CA).

Z′ factor and signal-to-noise (S/N) ratio are calculated according to the following formulas:

$$Z' = 1 - 3 * \frac{SD1 + SD2}{Abs(Av1 - Av2)} \tag{1}$$

$$\frac{S}{N} = \frac{Abs(Av1 - Av2)}{\sqrt{(SD1 * SD1 + SD2 * SD2)}} \tag{2}$$

Results and Discussion

Assay Development Scheme: How and Why?

The objective of this assay development was to develop a microplate-based in vitro high-throughput assay that can be used for the discovery of and screening for small-molecule radiation protectors and radiation mitigators in endothelium upon radiation damage.

Current epithelial cell-based models for radiation damage detection use hCMEC/D3 and HUVECs, and in some cases, bovine aortic endothelial cells (BAOECs) are also used to evaluate radiation damage. In this report, hCMEC/D3 cells and HUVECs were used as cell-based in vitro models; the hCMEC/D3 cell line was used for its availability and ease of use, and primary HUVECs were used for their human relevance.

The phenotypic assays were intentionally picked for major assay development based on the earlier observation of the transient cell size changes when irradiated. The choice of the phenotypic assays also reflects the uncertainty of molecular mechanisms of action, especially the dose-dependent and time-related mechanisms and responses. There have been reports on target-based assays for radiation responses, for example, DNA damage based; mitotic catastrophe and mitotic death; apoptosis, necrosis, and senescence; necroptosis and ferroptosis; and bystander effect (e.g., immunogenic cell death). However, no dominant factor has yet been identified that correlates well with the radiation cellular effects. Thus, for this project, the phenotypic assay development was the major direction we chose.

Our hypothesis for working with a phenotypic assay (**Fig. 1**) was that the radiation caused acute cellular responses (<24 h) as well as chronic responses (from 24 h to 7days), and the additional effects of rescuers/sensitizers were observed respectively. The responses of radiation were time-dependent, irradiation dose-dependent, and rescuer/sensitizer dose-dependent. Briefly, live-cell imaging was performed where acute responses were monitored with ~2–4 h intervals for the first 24 h (day 1), followed by 24 h intervals up to 7 days (day 7), to detect acute and chronic postirradiation responses (i.e., short-term and long-term effects) using
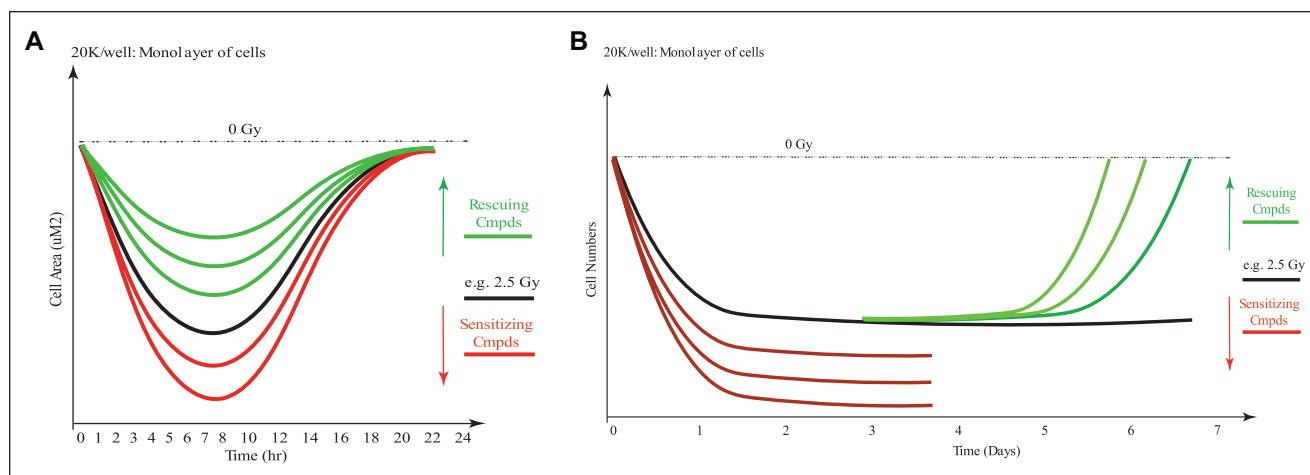
Figure 1. Hypothesis of acute and chronic responses of cells upon irradiation. (**A**) Schematic early time responses (<24 h) with cell area (or others). Green, rescuing compounds with increasing dose upward; red, sensitizing compounds with increasing dose downward; black, radiation effect without compounds. (**B**) Schematic long-term time responses (<7 days) with cell number (or others). Green, rescuing compounds with increasing dose upward; red, sensitizing compounds with increasing dose downward; black, radiation effect without compounds. 20K cells/well of hCMEC/D3 cells was used for the monolayer formation within the experimental time frame. The radiation dose (e.g., 2.5 Gy) was picked arbitrarily from the experiments. See article online for color figures.

label-free DPC imaging. Usually at the endpoints of both cases, the same plate was used to further quantify the phenotypes of radiation using nuclear, live-cell, and dead-cell staining. Both rescuing and sensitizing compounds (control compounds tested) in the acute phase (<24 h) and the chronic phase (up to 7 days) can be monitored by the transient phenotypes of cell numbers, cell area (μm^2), cell roundness, and contrast of DPC, as well as by endpoint cell staining results (among other parameters tested). These efforts were to explore and discover the optimal parameters (time and phenotypes) for the rescuing/mitigating compound responses. Both well-based image analysis and single cell-based image analysis were used for the characterization/optimization of the irradiation and drug effects.

To validate our hypothesis of the phenotypic assay, we designed the experiment as summarized in **Supplemental Scheme S1**. Multiple parameters of phenotypes in the cellular responses of irradiation were explored for correlation with the radiation doses. The radiation dose rates, the irradiation doses at the same dose rate, two cell line models (mainly hCMEC/D3 with further validation with HUVECs), and 11 different control compounds (**Fig. 2**) in serial dilution were systematically interrogated to try to develop the optimal robust assays for the effect of radiation.

The control compounds (**Fig. 2**) used as positive or negative controls tested in dose responses in the phenotypic assays were from the five categories of reported irradiation rescuing effects: (1) antioxidants or anti-inflammatory drugs (e.g., auranofin,[18] GC1149,[19] or Mito-TEMPO[20]); (2) OGG activators (e.g., V028-5832[21] or melatonin[22]); (3) GPX4 activators through ferroptosis (Y600-0815[23] or

($\pm$)-α-tocopherol acetate[24] as a vitamin E analog); (4) hits/leads from whole-animal irradiation experiments (e.g., recilisib sodium,[17] also known as Ex-Rad, and γ-tocotrienol[25]); and (5) others, for example, HDAC inhibitors (trichostatin A[26]). Dactinomycin and piplartine were used as negative controls or sensitizer controls.

The assay development workflow (**Suppl. Scheme S2**) was designed to achieve the following objectives: (1) Determine the maximum window of signals for the phenotypes and the maximal irradiation doses (up to 444 Gy at 22.2 Gy/min). Earlier trials with low doses (<10 Gy) of irradiation have shown only minimal, if any, postirradiation signal. The maximum windows of signals were found to be time point-dependent. (2) Optimize the radiation doses to observe the dose responses of the phenotypes (enough irradiation signal windows) to interrogate control compound effects, that is, to generate dose responses of rescuing/mitigating or sensitizing controls. (3) Reduce radiation doses to find optimal conditions (doses and time points) for rescuing/mitigating control compounds, preferably with the highest Z′ factor or optimal dose responses of the controls to ensure assay robustness. This reduction of radiation doses will also be used to accommodate the different mechanisms of action for low-dose irradiation.

The results from this workflow, experimental design, and timeline are discussed separately in the following sections.

Radiation Doses and Cellular Responses

For the development of our in vitro plate-based assay, the maximum radiation dose up to 444 Gy at 22.2 Gy/min was
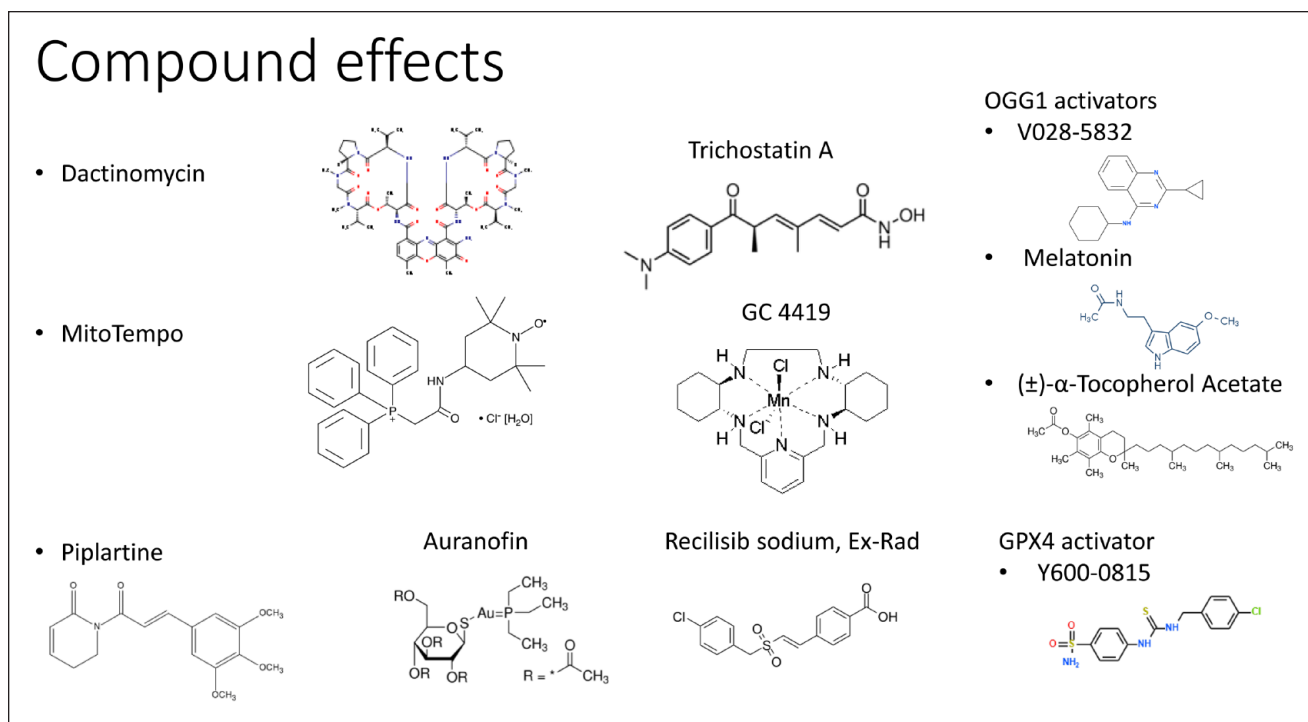
Figure 2. Representative control compounds tested in dose responses in the phenotypic assay development as positive or negative controls to evaluate the assay responses.
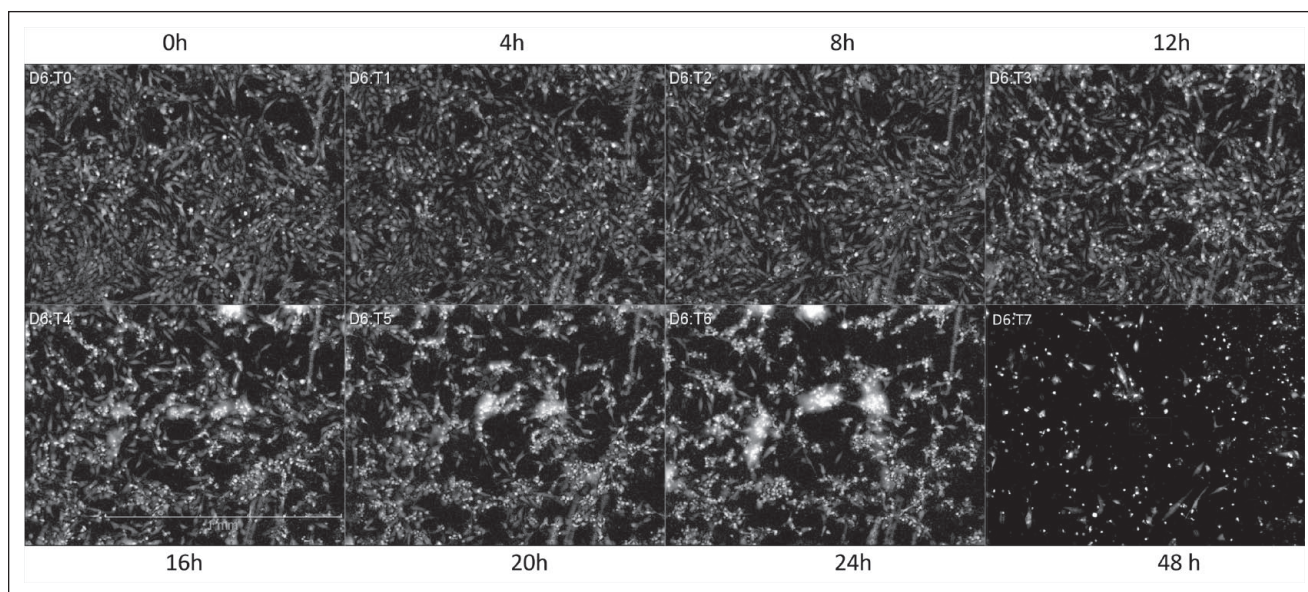

Figure 3. Images (DPC) for the time-course of hCMEC/D3 cells with a 444 Gy dose of irradiation at 22.2 Gy/min. Seeding in 20K/well, monitored for 2 days postirradiation.

applied to the hCMEC/D3 cells. Representative live-cell imaging of the time-course responses upon irradiation is shown in **Figure 3**. The label-free DPC imaging of the plate provided the time-dependent phenotypical changes in cell numbers, cell area, cell roundness, and cell contrast of DPC intensity.

The radiation dose effects on the cells were further studies at four different doses at the same dose rate of 22.2 Gy/
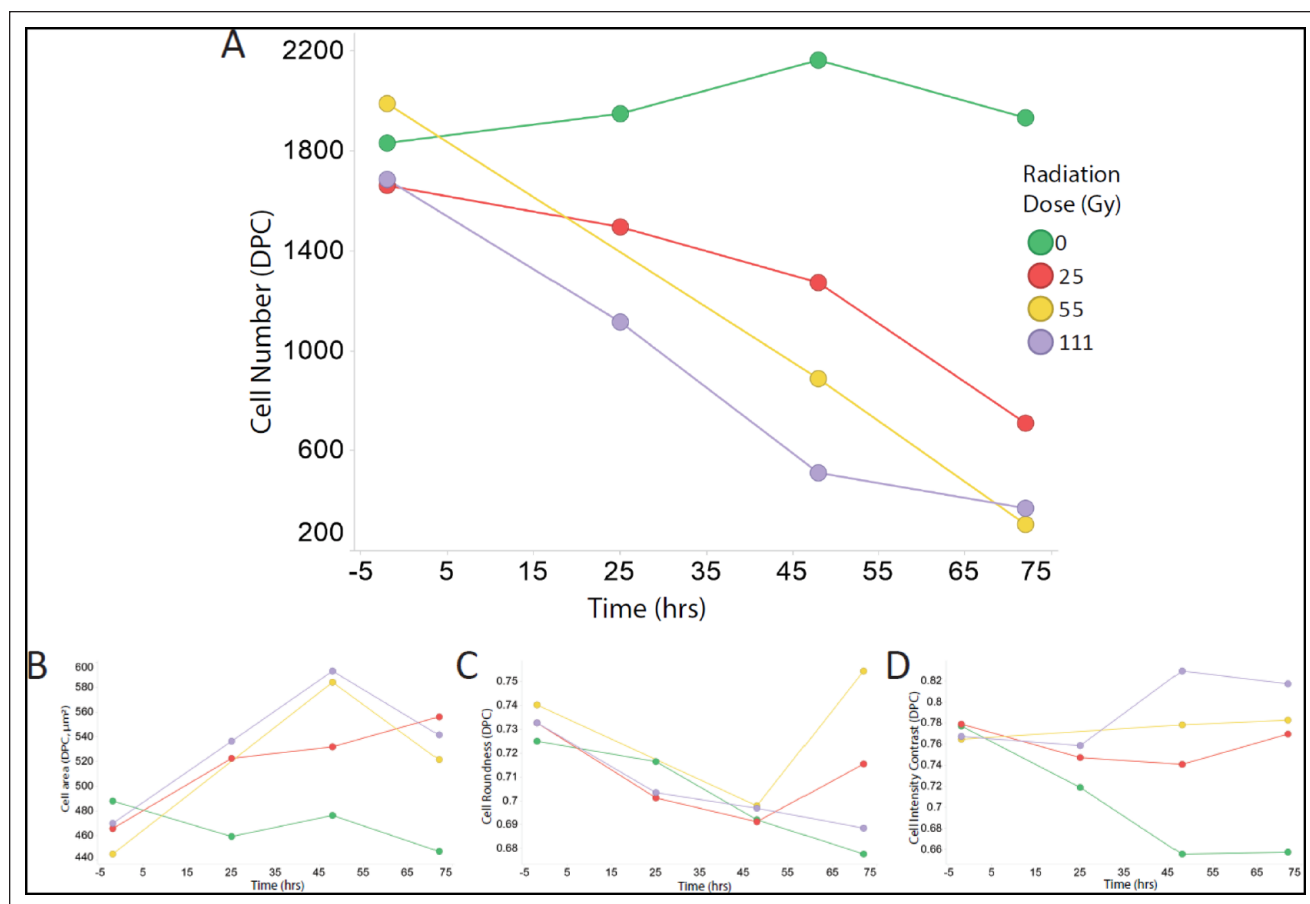
Figure 4. Radiation dose responses of the endothelial cells in a 72 h time-course. (**A**) Cell numbers in doses of 0 (green), 25 (red), 55 (yellow), and 111 (purple) Gy at 22.2 Gy/min. (**B**) Cell area (μm^2) in doses of 0 (green), 25 (red), 55 (yellow), and 111 (purple) Gy at 22.2 Gy/min. (**C**) Cell roundness in doses of 0 (green), 25 (red), 55 (yellow), and 111 (purple) Gy at 22.2 Gy/min. (**D**) Cell DPC intensity contrast in doses of 0 (green), 25 (red), 55 (yellow), and 111 (purple) Gy at 22.2 Gy/min. hCMED/D3 cells in 20K/well, monitored for 2 days after irradiation. See article online for color figures.

min at a seeding density of 20K/well (monolayer formation). The postirradiation cell response over 72 h is summarized in **Figure 4**. The cell number responses postirradiation are shown in **Figure 4A**; as the irradiation increased from 0 Gy to 111 Gy, the cell number decreased accordingly up to 72 h. The cell area (μm^2), cell roundness, and cell DPC intensity contrast upon irradiation at 0, 25, 55, and 111 Gy are shown in **Figure 4B–D**, respectively. All of them showed radiation dose-dependent changes.

Radiation Doses and Control Drug Dose Responses

The effects of six control compounds (auranofin, dactinomycin, GC1149, Mito-TEMPO, recilisib sodium, and trichostatin A) in serial dilutions were tested at four different radiation doses at the same dose rate of 22.2 Gy/min (**Fig. 5**). At 0 Gy irradiation, auranofin, dactinomycin, and trichostatin A already had dose responses on inducing cell

death. With increasing radiation doses, these three compounds had similar potencies (IC_{50} values) but increasing efficacy of inducing cell death. They can be considered as irradiation sensitizers (**Fig. 5A**). GC1149, Mito-TEMPO, and recilisib sodium had no effect on cells in 0 Gy. No dose responses from these three compounds were observed in increasing radiation doses, merely only the irradiation effect itself with the time-course responses. Marginal protection was observed in the low-concentration range for these control compounds (<0.1 μM), although this result was not reproducible.

The postirradiation effects of these six control compounds on other phenotypes, including cell area (μm^2), cell roundness, and cell DPC intensity contrast, are shown in **Figure 5B–D**, respectively. Similar results were also observed for auranofin, dactinomycin, and trichostatin A, along with GC1149, Mito-TEMPO, and recilisib sodium. No significant protection was detected with the potential rescuing/mitigating molecules.
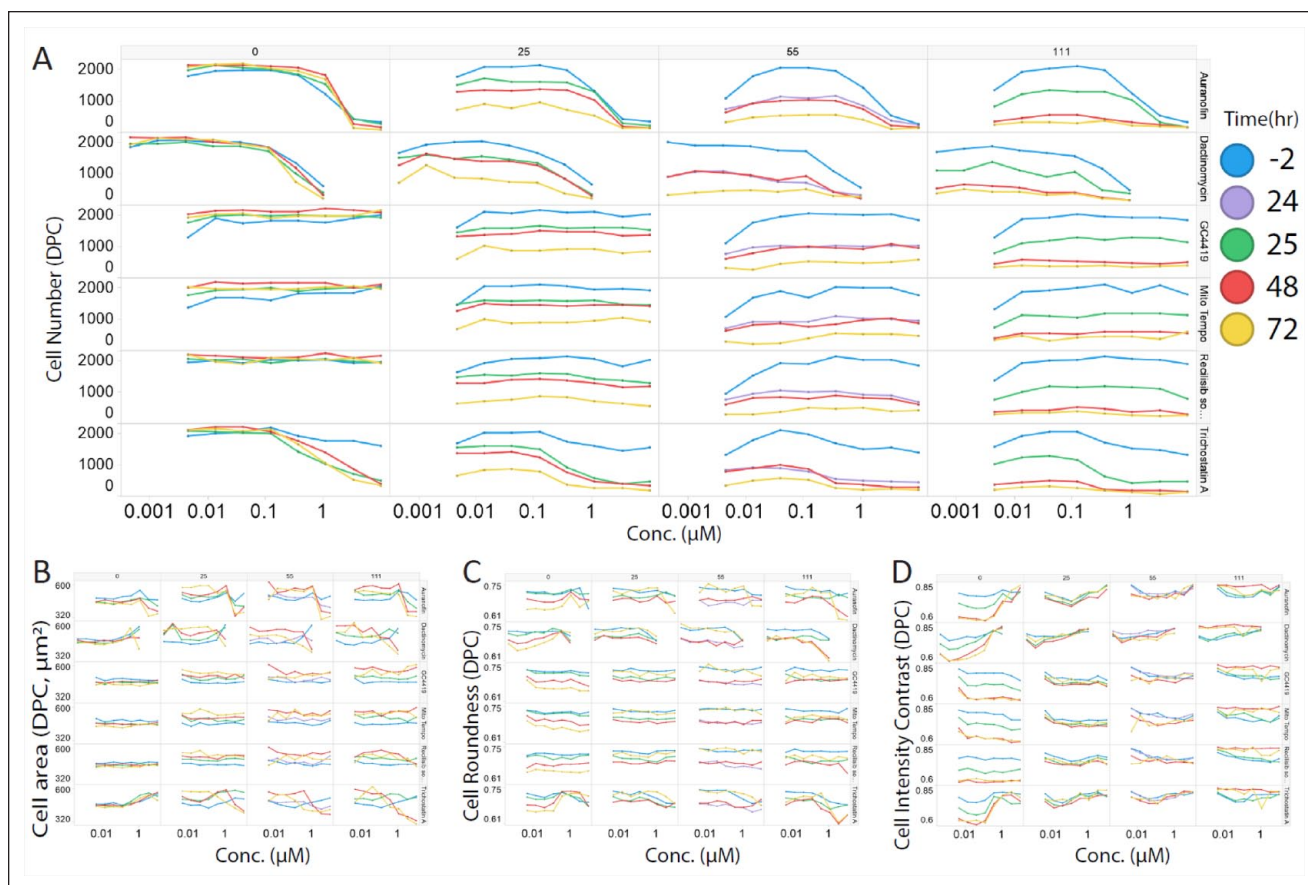
Figure 5. Compound effects (dose responses) in different radiation doses. (**A**) Cell numbers in different time points: −2 h (blue), 24 h (purple), 25 h (green), 48 h (red), and 72 h (yellow). Top: Irradiation doses at 0, 25, 55, abd 111 Gy at 22.2 Gy/min. Right vertical: Compound names: auranofin, dactinomycin, GC1149, Mito-TEMPO, recilisib sodium, and trichostatin A. (**B**) Cell area (µm^2) in 0 (green), 25 (red), 55 (yellow), and 111 (purple) Gy at 22.2 Gy/min. (**C**) Cell roundness in 0 (green), 25 (red), 55 (yellow), and 111 (purple) Gy at 22.2 Gy/min. (**D**) Cell DPC intensity contrast in 0 (green), 25 (red), 55 (yellow), and 111 (purple) Gy at 22.2 Gy/min. hCMED/D3 cells in 20K/well, monitored for 2 days after irradiation. See article online for color figures.

The effect of the radiation doses on the cell numbers for control compounds (**Fig. 6**) demonstrates a radiation dose-dependent relationship. At 10 Gy, most of the compounds reached >80% cell death at 72 h. Hence, 10 Gy was used for later experiments with the rescuing/mitigating molecule assay.

The timing of the application of the small-molecule rescuers/mitigators in all experiments is intentionally set at 24 h before irradiation. This timing could maximize the drug effect (protection or sensitization) in the cells in combination with serial doses of the drugs. This could minimize the effect of timing by covering all possible scenarios with diverse concentrations instead of a single concentration. There was no drug in the cell anymore after irradiation. All the effects are due to the downstream effects of the drugs before irradiation. This is also intentionally correlated with potential clinical application to eliminate radiation side effects before treatment. Application after irradiation was

not explored at this time because the different drugs might take different lengths of time to be effective and might induce further compound effects for result interpretation.

Nonlinear Cell Responses and Irradiation Doses

It has been established that the postirradiation noxious effects to cells and tissue are nonlinear at low and high doses,[28] arbitrarily separated at around 0.1 Gy, based on epidemiology studies (**Suppl. Scheme S3A**).[29,30] Several non-extrapolatable effects have been reported, including a bystander effect,[31] linear extrapolation, adaptive responses,[32] and hormesis,[33] with different kinds of mechanisms of action at low doses. Especially important for this project is the discovery for radiation rescue/mitigation, which is usually in the loosely defined low-dose range. For this consideration, the radiation dose has to be intentionally set at less than 10 Gy to have enough possibility to be rescued/
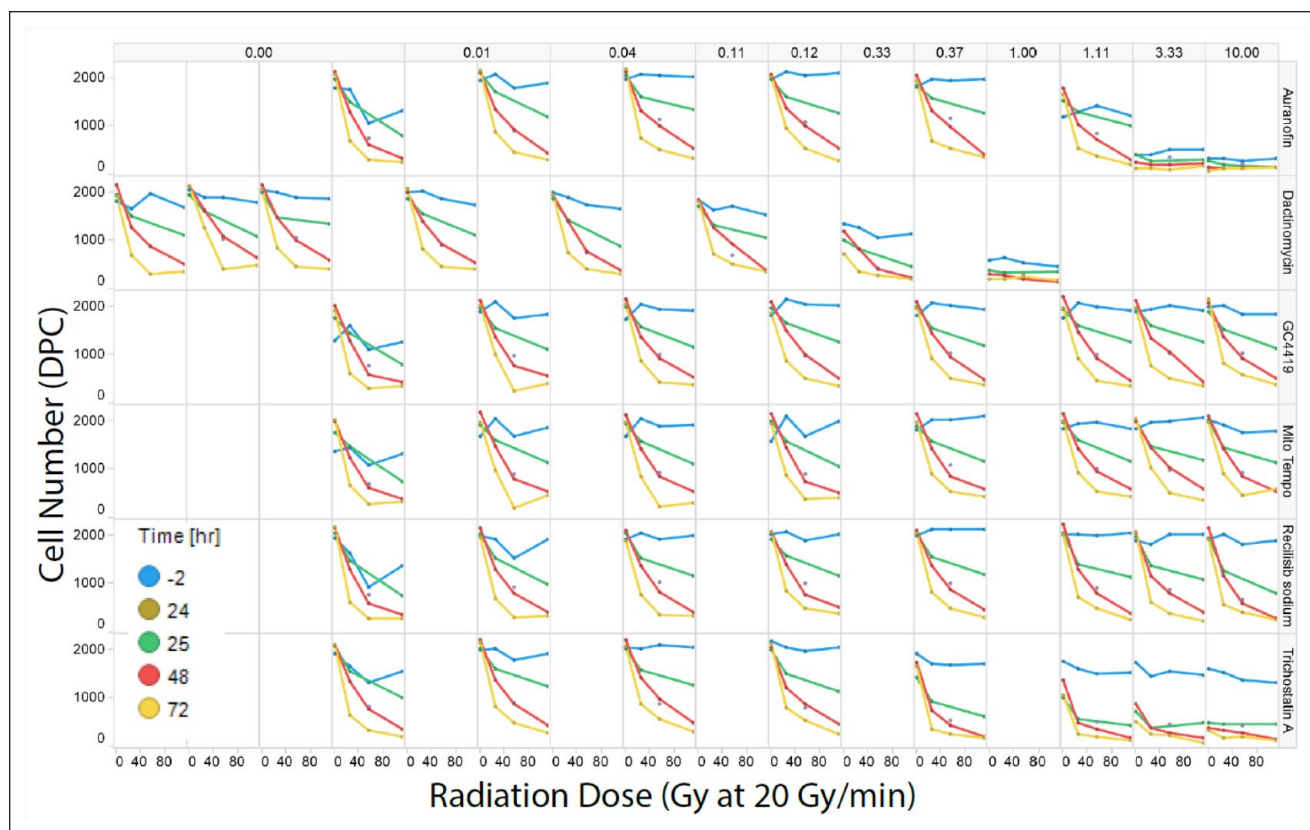
Figure 6. Radiation dose effects with different drug controls and time-course responses. Top: Control drug concentrations (μM). Right vertical: Compound names: auranofin, dactinomycin, GC1149, Mito-TEMPO, recilisib sodium, and trichostatin A. hCMED/D3 cells in 20K/well, monitored for 2 days after irradiation. See article online for color figures.

mitigated by the small-molecule compounds. Otherwise, the rescuing/mitigating effects of the small molecules (in others as well) could not be detected due to higher radiation damages. Alternatively, too low irradiation doses would limit the window of the signal and potentially the robustness of the assay. The nonlinearity of the radiation dose effects eliminates the possibility of using higher radiation doses for larger signal windows, with extrapolation back to low radiation doses.

Furthermore, the bystander effect (**Suppl. Scheme S3B**)[34] is also an important mechanism for the low irradiation effect for cell-to-cell interactions. The direct-hit cells and non-direct-hit cells (hence "bystander") form two distinct populations of cells that not only have unique responses to radiation, but also introduce downstream cell signaling responses through cell–cell tight junctions and intercellular signaling. By controlling cell density, the direct-hit cell population can be identified using low cell density, whereas both direct-hit and non-direct-hit cell populations can be detected using a monolayer of cells. In this report, we used a monoculture of epithelial cells, but multiculture cellular models are available to observe more complicated bystander effects.

The postirradiation effects of the cell density and different cell monocultures (hCMEC/D3 and HEC-50) were tested (**Fig. 7**). hCMEC/D3 cells, an epithelial cell line, did show cell density-dependent responses. This is displayed by the DPC response (increasing DPC cell number), DPC intensity (increasing contrast), Hoechst nuclei staining (increasing nuclei number), ethidium homodimer for dead cells (increasing dead cells), and calcein-AM for live cells (not many live cells) at a 444 Gy irradiation dose. In contrast, HEC-50, an endometrial cancer cell line, has shown the DPC response (increasing DPC cell number), DPC intensity (increasing contrast), Hoechst nuclei staining (increasing nuclei number), ethidium homodimer for dead cells (decreasing dead cells), and calcein-AM for live cells (increasing live cells) at an irradiation dose of 444 Gy.

Irradiation Rescuing/Mitigating Molecule Assays

Based on the abovementioned optimization of radiation doses, cell density, and time-course responses from acute (<24 h) and chronic (up to 7 days) phases, we further tested irradiation doses of less than 10 Gy with reported radiation
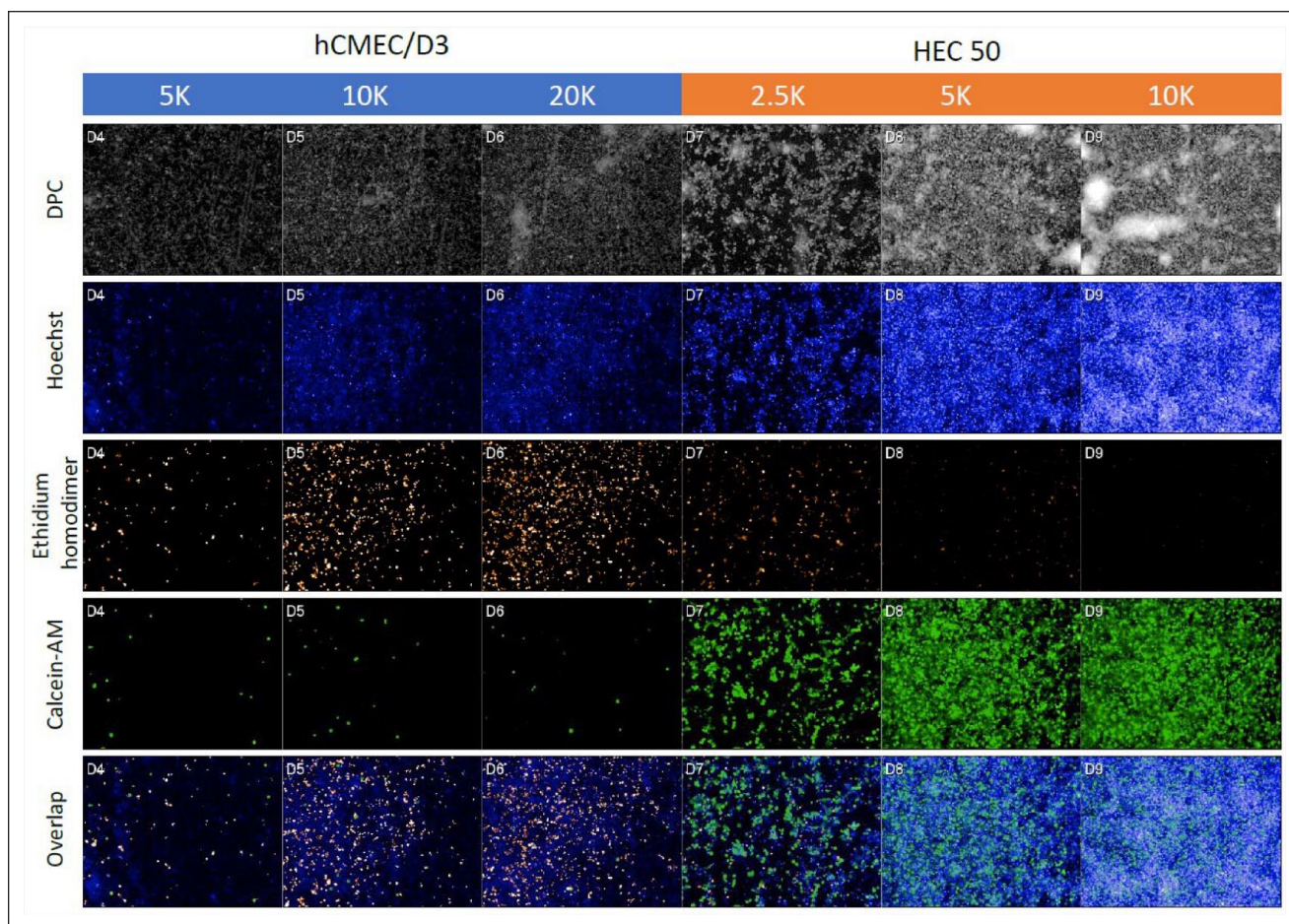
Figure 7. Cell density effects of hCMEC/D3 and HEC-50 cells upon irradiation by 444 Gy at 22 Gy/min at the 72 h time point. The cells at different cell densities were stained with Hoechst for nuclei, calcein-AM for live-cell staining, and ethidium homodimer for dead-cell staining. DPC was used for label-free cell staining.

rescuing control compounds and live-cell, time-course imaging.

As for the acute radiation effect (<24 h) at 2.5 Gy, there were no significant effects on the cell number (**Suppl. Fig. S8**) for all tested control compounds (dactinomycin, Mito-TEMPO, V028-5832, Y600-0815, melatonin, and (±)-α-tocopherol acetate in serial dilutions), except for dactinomycin, a known cell-killing drug (top row). Other parameters of postirradiation effects, that is, cell area (μm^2), cell roundness, and cell DPC intensity contrast, were similar for these six control compounds (**Suppl. Fig. S9**). Cell density effects were also observed, with dactinomycin having more potency/efficacy in lower cell seeding density (5000 cells/well) than in higher (monolayer forming, 20,000 cells/well).

As for the chronic radiation effect (up to 7 days) with the same plate map with 0, 2.5, 5, and 10 Gy/plate of irradiation, only dactinomycin demonstrated dose responses with increasing efficacy in cell number changes with increasing

irradiation doses (**Suppl. Fig. S10**). Other parameters of postirradiation effects, that is, cell area (μm^2), cell roundness, and cell DPC intensity contrast, were similar for these six control compounds (**Suppl. Fig. S11**).

No dose responses were observed in both acute and chronic irradiation effects, with five reported rescuing control compounds in serial dilution and four different doses of "low-dose" irradiation.

Based on these results, we decided not to proceed with the pilot screening for the following considerations: (1) With the current phenotypic assay approach, we could not generate a dose response with the control compounds, even though some reported rescuing molecules have already been tested in vivo and in some clinical trial cases.[35] (2) Multiple mechanisms of action, especially in the low-dose irradiation condition, might not generate enough of a signal window to produce the necessary cellular phenotypes for irradiation rescuing/mitigating compounds. (3) For low-dose irradiation, the signal window is too small to be

considered for physiological relevance. Despite our efforts, we were not able to determine the optimal radiation dose. Radiation doses that were too low resulted in a small signal, and those that were too high (or even at a medium-high level) raised concerns about the relevance by extrapolation and difficulty of the rescue.

We are reporting this failed assay to demonstrate that even with much effort and a strong rationale supporting the different conditions tested, the signal window can still be limited to the extent that it does not generate a robust assay for potential screening effects. These lessons learned fall into the category of the proverbial valley of death often encountered in assay development, which can also be similar to the challenges experienced during clinical trials: (1) phenotypic assays are not exactly physiologically relevance, and (2) target-based assays are not necessarily correlated to phenotypic observations. The different kinds of targets discussed above can only be considered as related, but not correlated, especially when the kinetic time-course measurement is used. To overcome these valleys of death in assay development, more thorough systematic approaches are needed to bridge the gap between assays and phenotypes, similar to the efforts in this failed assay. In addition, there is a need to target the responses required to facilitate screening efforts that allow for the discovery of in vivo and preferably clinical trial-relevant hits, which can eventually lead to therapeutics.

Despite the "failed" development of phenotypic assays for irradiation rescue of compounds in this report, we are still working on alternative assays: (1) target-based assays based on the low-dose mechanisms of action, for example, irradiation-induced direct DNA damage level and recovery, mitochondrial DNA damage and recovery, and reactive oxygen species and nitric oxide synthase as cellular signaling pathways for both direct-hit cells and bystander cells; (2) better in vitro cellular models for irradiation effects, such as the transwell systems for irradiation-induced leaking of epithelial monolayers, wound-healing functional models for epithelial cells, and 3D organ-on-a-chip models for epithelium (e.g., MIMETAS system); and (3) innate immune responses upon irradiation as well as co-culture immune responses for irradiation effects.

Acknowledgments

Declaration of Conflicting Interests

Funding

ORCID iD

Meng Wu https://orcid.org/0000-0003-2222-0736

References

1. Markossian, S.; Sittampalam, G.; Grossman, A.; et al. *Assay Guidance Manual*. Eli Lilly & Company and the National Center for Advancing Translational Sciences: Bethesda, MD, 2004–.

2. Parrish, M. C.; Tan, Y. J.; Grimes, K. V.; et al. Surviving in the Valley of Death: Opportunities and Challenges in Translating Academic Drug Discoveries. *Annu. Rev. Pharmacol. Toxicol*. **2019**, *59*, 405–421.

3. Gamo, N. J.; Birknow, M. R.; Sullivan, D.; et al. Valley of Death: A Proposal to Build a "Translational Bridge" for the Next Generation. *Neurosci. Res*. **2017**, *115*, 1–4.

4. Inglese, J.; Johnson, R. L.; Simeonov, A.; et al. High-Throughput Screening Assays for the Identification of Chemical Probes. *Nat. Chem. Biol*. **2007**, *3*, 466–479.

5. Nikolic, M.; Sustersic, T.; Filipovic, N. In Vitro Models and On-Chip Systems: Biomaterial Interaction Studies with Tissues Generated Using Lung Epithelial and Liver Metabolic Cell Lines. *Front. Bioeng. Biotechnol*. **2018**, *6*, 1–13.

6. Nikolakopoulou, P.; Rauti, R.; Voulgaris, D.; et al. Recent Progress in Translational Engineered In Vitro Models of the Central Nervous System. *Brain* **2020**, *143*, 3181–3213.

7. Sittampalam, G. S.; Iversen, P. W.; Boadt, J. A.; et al. Design of Signal Windows in High Throughput Screening Assays for Drug Discovery. *J. Biomol. Screen*. **1997**, *2*, 159–169.

8. Wang, G. A.; Xie, X.; Mansour, H.; et al. Expanding Detection Windows for Discriminating Single Nucleotide Variants Using Rationally Designed DNA Equalizer Probes. *Nat. Commun*. **2020**, *11*, 5473–5484.

9. Lage, O. M.; Ramos, M. C.; Calisto, R.; et al. Current Screening Methodologies in Drug Discovery for Selected Human Diseases. *Mar. Drugs* **2018**, *16*, 279–310.

10. Moffat, J. G.; Vincent, F.; Lee, J. A.; et al. Opportunities and Challenges in Phenotypic Drug Discovery: An Industry Perspective. *Nat. Rev. Drug Discov*. **2017**, *16*, 531–543.

11. Baskar, R.; Lee, K. A.; Yeo, R.; et al. Cancer and Radiation Therapy: Current Advances and Future Directions. *Int. J. Med. Sci*. **2012**, *9*, 193–199.

12. Arina, A.; Gutiontov, S. I.; Weichselbaum, R. R. Radiotherapy and Immunotherapy for Cancer: From "Systemic" to "Multi-Site." *Clin. Cancer Res*. **2020**, 2034–2019.

13. Dilalla, V.; Chaput, G.; Williams, T.; et al. Radiotherapy Side Effects: Integrating a Survivorship Clinical Lens to Better Serve Patients. *Curr. Oncol*. **2020**, *27*, 107–112.

14. Wittig, A.; Engenhart-Cabillic, R. Cardiac Side Effects of Conventional and Particle Radiotherapy in Cancer Patients. *Herz* **2011**, *36*, 311–324.

15. Hufnagle, J. J.; Goyal, A.; Maani, E. V. Radiation Therapy Induced Cardiac Toxicity. In: *StatPearls* [Internet]; **2021**. https://www.ncbi.nlm.nih.gov/books/NBK554453/ (accessed June 1, 2021).

16. Grumbach, I. M. Cardio-Oncology at the Beginning of a New Decade. *J. Am. Heart Assoc*. **2020**, *9*, e015890.

17. Kang, A. D.; Cosenza, S. C.; Bonagura, M.; et al. ON01210. Na (Ex-RAD®) Mitigates Radiation Damage through Activation of the AKT Pathway. *PLoS One* **2013**, *8*, e58355.

18. Nag, D.; Bhanja, P.; Riha, R.; et al. Auranofin Protects Intestine against Radiation Injury by Modulating p53/p21 Pathway and Radiosensitizes Human Colon Tumor. *Clin. Cancer Res*. **2019**, *25*, 4791–4807.

19. Mapuskar, K. A.; Anderson, C. M.; Spitz, D. R.; et al. Utilizing Superoxide Dismutase Mimetics to Enhance Radiation Therapy Response While Protecting Normal Tissues. *Semin. Radiat. Oncol*. **2019**, *29*, 72–80.

20. Kim, S.; Choe, J. H.; Lee, G. J.; et al. Ionizing Radiation Induces Innate Immune Responses in Macrophages by Generation of Mitochondrial Reactive Oxygen Species. *Radiat. Res*. **2016**, *187*, 32–41.

21. Baptiste, B. A.; Katchur, S. R.; Fivenson, E. M.; et al. Enhanced Mitochondrial DNA Repair of the Common Disease-Associated Variant, Ser326Cys, of hOGG1 through Small Molecule Intervention. *Free Radic. Biol. Med*. **2018**, *124*, 149–162.

22. Rezapoor, S.; Shirazi, A.; Abbasi, S.; et al. Modulation of Radiation-Induced Base Excision Repair Pathway Gene Expression by Melatonin. *J. Med. Phys*. **2017**, *42*, 245–250.

23. Li, C.; Deng, X.; Zhang, W.; et al. Novel Allosteric Activators for Ferroptosis Regulator Glutathione Peroxidase 4. *J. Med. Chem*. **2019**, *62*, 266–275.

24. Singh, P. K.; Krishnan, S. Vitamin E Analogs as Radiation Response Modifiers. *Evid. Based Complement. Alternat. Med*. **2015**, *2015*, 741301.

25. Satyamitra, M.; Ney, P.; J Graves, I.; et al. Mechanism of Radioprotection by δ-Tocotrienol: Pharmacokinetics, Pharmacodynamics and Modulation of Signalling Pathways. *Br. J. Radiol*. **2012**, *85*, e1093–e1103.

26. Nagarajan, D.; Wang, L.; Zhao, W.; et al. Trichostatin A Inhibits Radiation-Induced Epithelial-to-Mesenchymal Transition in the Alveolar Epithelial Cells. *Oncotarget* **2017**, *8*, 101745–101759.

27. Landauer, M. R.; Harvey, A. J.; Kaytor, M. D.; et al. Mechanism and Therapeutic Window of a Genistein Nanosuspension to Protect against Hematopoietic-Acute Radiation Syndrome. *J. Radiat. Res*. **2019**, *60*, 308–317.

28. Bonner, W. M. Low-Dose Radiation: Thresholds, Bystander Effects, and Adaptive Responses. *Proc. Natl. Acad. Sci. U.S.A*. **2003**, *100*, 4973–4975.

29. Ono, T.; Grodzinsky, D. Scientific Risk Estimation on Health Effects of Low Dose and Low Dose-Rate Radiation—An Overview. *Data Sci. J*. 2009, *8*, BR1–BR4.

30. Picano, E.; Vano, E. The Radiation Issue in Cardiology: The Time for Action Is Now. *Cardiovasc. Ultrasound* **2011**, *9*, 35.

31. Hu, S.; Shao, C. Research Progress of Radiation Induced Bystander and Abscopal Effects in Normal Tissue. *Radiat. Med. Prot*. **2020**, *1*, 69–74.

32. Guéguen, Y.; Bontemps, A.; Ebrahimian, T. G. Adaptive Responses to Low Doses of Radiation or Chemicals: Their Cellular and Molecular Mechanisms. *Cell. Mol. Life Sci*. **2019**, *76*, 1255–1273.

33. Luckey, T. D. Radiation Hormesis: The Good, the Bad, and the Ugly. *Dose Response* **2006**, *4*. DOI: dose-response.06-102. Luckey.

34. Matsuya, Y.; Sasaki, K.; Yoshii, Y.; et al. Integrated Modelling of Cell Responses after Irradiation for DNA-Targeted Effects and Non-Targeted Effects. *Sci. Rep*. **2018**, *8*, 4849.

35. Oronsky, B.; Goyal, S.; Kim, M. M.; et al. A Review of Clinical Radioprotection and Chemoprotection for Oral Mucositis. *Transl. Oncol*. **2018**, *11*, 771–778.